Available online at www.sciencedirect.com
ScienceDirect
Polymer 48 (2007) 3850–3857
polymer
www.elsevier.com/locate/polymer

Solid-state ^{13}C NMR investigation of the structure and hydrogen bonding for stereoregular poly(vinyl alcohol) films in the hydrated state

Hiroyuki Ohgi [a,*], Hu Yang [b,1], Toshiaki Sato [a], Fumitaka Horii [b]

[a] *Tsukuba Research Laboratories, Kuraray Co., Ltd., 41, Miyukigaoka, Tsukuba, Ibaraki 305-0841, Japan*
[b] *Institute for Chemical Research, Kyoto University, Uji, Kyoto 611-0011, Japan*

Received 2 December 2006; received in revised form 3 April 2007; accepted 15 April 2007
Available online 19 April 2007

Abstract

The structure and hydrogen bonding of the hydrated stereoregular poly(vinyl alcohol) (PVA) films have been investigated by high-resolution solid-state ^{13}C NMR spectroscopy. It is found by the ^{13}C spin-lattice relaxation analysis that there exist three components with different T_{1C} values assigned to the crystalline, less mobile and mobile components for the hydrated syndiotactic PVA (S-PVA) and highly isotactic PVA (HI-PVA) films. The line shape analysis indicates that the probability of intramolecular hydrogen bonding is appreciably increased in the crystalline region for the S-PVA films by the hydration but a slightly helical structure, which is probably allowed by the formation of the successive intramolecular hydrogen bondings along the chains in the crystalline region, seems not to undergo any significant change by the hydration for HI-PVA. This fact indicates that intramolecular hydrogen bonding is more stable in the hydrated state in the crystalline region. As for the less mobile component, the line shape of the CH resonance line for the hydrated S-PVA or HI-PVA films is found to be very similar to that of the corresponding crystalline component, probably being due to the successive formation of intermolecular or intramolecular hydrogen bonding in the interfacial region, which mainly contributes to the less mobile component, for the S-PVA or HI-PVA films even in the hydrated state. The mole fractions of the *mm*, *mr* and *rr* sequences are also estimated for the mobile component that is produced in each stereoregular PVA sample by swelling with water and it is concluded that no prominent preferential partitioning of the *mm*, *mr* and *rr* sequences occurs in the crystalline and noncrystalline regions for the PVA films with different tacticities.

Keywords: Stereoregular poly(vinyl alcohol); Hydrogen bonding; CP/MAS ^{13}C NMR

1. Introduction

Many investigations have been reported on the synthesis of stereoregular poly(vinyl alcohol)s (PVAs) being rich in syndiotactic or isotactic sequences [1–3]. A marked dependence of stereoregularity on their properties has been recognized, which may be mainly caused by difference in inter- and intramolecular hydrogen bondings. Irrespective of many efforts paid to prepare stereoregular PVAs as reported previously [4–9], the stereoregularity still remained at a low level of the *mm* fraction (=0.70) even for so-called isotactic PVA (LI-PVA) derived from poly(trimethyl silyl vinyl ether) [9,10]. Recently, we studied the cationic polymerization of *t*BVE with boron trifluoride diethyl etherate ($BF_3 \cdot OEt_2$) and successfully prepared the PVAs having the highest isotacticity so far reported [10–12]. We found interesting features of these highly isotactic PVAs (HI-PVAs) being different from those of LI-PVA and ordinary atactic PVA (A-PVA) [10,13,14]. In particular, we compared the melting temperatures T_m, degrees of crystallinity χ_c, and ^{13}C spin-lattice relaxation times T_{1C} of the crystalline components for PVA samples with different tacticities (including HI-PVA) to find that these physical quantities show clear minima at the *mm* fraction = 0.4–0.5 when

* Corresponding author. Tel.: +81 29 853 1521; fax: +81 29 853 1543.
E-mail address: hiroyuki_ogi@kuraray.co.jp (H. Ohgi).
[1] Present address: School of Chemistry and Chemical Engineering, Nanjing University, Nanjing 210093, People's Republic of China.

0032-3861/$ - see front matter © 2007 Elsevier Ltd. All rights reserved.
doi:10.1016/j.polymer.2007.04.023

plotted against *mm* [14]. This result suggests that the structural disordering associated with the decrease in the crystallinity occurs most significantly in this *mm* range. In relation to these minima, FTIR spectroscopy confirmed the formation of the new crystal form for HI-PVAs with $mm > 0.55$ and solid-state ^{13}C NMR spectroscopy revealed that all OH groups are allowed to form successive intramolecular hydrogen bonding along the respective chains in the crystalline region for HI-PVAs with $mm > 0.7$.

As described above, the solid-state ^{13}C NMR analyses are powerful for the characterization of hydrogen bonding of PVA in the solid state. On the other hand, the characterization of hydrogen bonding in the hydrated state of PVA should be also very important, because the characteristic properties and functions of some applications of PVA, i.e. hydrogels, may greatly depend on their hydrogen-bonded states. In a previous paper [15], the hydration process and resulting hydrogen bonding for A-PVA films have been investigated by the solid-state ^{13}C NMR analysis. It was found that there were three components with different T_{1C} values assigned to the crystalline, less mobile, and mobile components in the hydrated A-PVA films. In the crystalline component, the probability f_a of the formation of intramolecular hydrogen bonding is significantly increased by the addition of water. In the less mobile component, two types of hydrogen bonds are found to still remain even in the presence of water but the *gauche* fraction greatly increases compared to the case in the dried state due to breaking of hydrogen bonding, and the mobile component is subjected to rapid exchanges among different conformations and hydrogen bonds. Moreover, the analysis of the mole fractions of the *mm*, *mr*, and *rr* sequences obtained for the mobile component indicates that the different triad structural units are almost equally distributed in the crystalline and noncrystalline regions for A-PVA.

In this paper, we apply similar ^{13}C NMR analyses to the characterization of the structure and hydrogen bonding for the hydrated HI-PVA and syndiotactic PVA (S-PVA) films. We also investigate the possibility of the partitioning of the different triad sequences into the crystalline and noncrystalline regions in these samples by selectively measuring the triad tacticities for the mobile components that are produced by swelling with water. The clarification of such partitioning is very important to understand the molecular motion in the noncrystalline region for stereoregular PVA samples in relation to the triad tacticity [16].

2. Experimental

2.1. Synthesis of stereoregular PVAs

Polymerization of *t*BVE was carried out with $BF_3 \cdot OEt_2$ in toluene at −78 °C, and the resulting polymer was converted into HI-PVA by the cleavage of the ether linkage using hydrogen bromide at 0 °C. A commercially available A-PVA derived from poly(vinyl acetate) and syndiotactic PVA (S-PVA) derived from poly(vinyl pivalate) by the method previously reported [17] were used as the reference materials to clarify unique, solid-state properties of HI-PVAs.

2.2. Determination of stereoregularity of PVAs

The stereoregularity of PVA samples was determined from solution-state ^1H NMR spectroscopy on the basis of the methods [18,19] reported previously. ^1H NMR spectra were measured in deuterated dimethyl sulfoxide (DMSO-d_6) at 25.0 °C on a JEOL GSX-270 spectrometer operating at 270.17 MHz. The triad tacticities are as follows: HI-PVA ($mm = 0.78$, $mr = 0.20$, $rr = 0.03$), A-PVA (0.23, 0.50, 0.27), S-PVA (0.14, 0.48, 0.38).

2.3. Preparation and hydration of PVA films

HI-PVA and S-PVA films were prepared by casting 5 wt% DMSO solutions on glass plates, allowing DMSO to evaporate at 50 °C for 20 h, immersing them in hot methanol overnight, and then drying in vacuum at room temperature for 2 days. The respective films were further subjected to annealing at 200 and 40 °C for 10 min under vacuum, respectively.

Hydrated stereoregular PVA films for solid-state ^{13}C NMR measurements were prepared by soaking the annealed PVA films in distilled water for 24 h, gently pressed with filter papers, and then packed into the MAS rotor with an O-ring seal [20,21] to avoid the loss of water during NMR measurements. The water contents were about 0.72 g-water/g-PVA for the hydrated HI-PVA films and about 0.80 g-water/g-PVA for the hydrated S-PVA films.

2.4. Solid-state ^{13}C NMR spectroscopy

Cross polarization/magic angle spinning (CP/MAS) ^{13}C NMR spectroscopy was performed at room temperature on a Chemagnetics CMX-200 spectrometer equipped with a JEOL CP/MAS probe, which was operating under a static magnetic field of 4.7 T. ^1H and ^{13}C radio-frequency field strengths $\gamma B_1/2\pi$ were 69 kHz in the CP process, whereas the ^1H field strength was reduced to 59 kHz for the dipolar decoupling. The CP contact time and MAS rate were set to 1 ms and 3.5 kHz, respectively. A MAS rotor with an O-ring seal [20,21] was employed for the dried or hydrated samples to keep the dried or hydrated state during NMR measurements. The detailed procedure of the solid-state ^{13}C NMR measurements was almost the same as described in the previous papers [15,21–26].

3. Results and discussion

3.1. Structure and hydrogen bonding of the hydrated films

Fig. 1a shows a fully relaxed dipolar decoupling (DD)/MAS ^{13}C NMR spectrum measured for the hydrated S-PVA films with a water content of 0.80 g-H_2O/g-PVA by the $\pi/4$ single sequence with a pulse delay time of 50 s. A sharp triplet is clearly observed for the CH resonance line and the constituent lines are assigned to the CH carbons in the *mm*, *mr* and *rr*

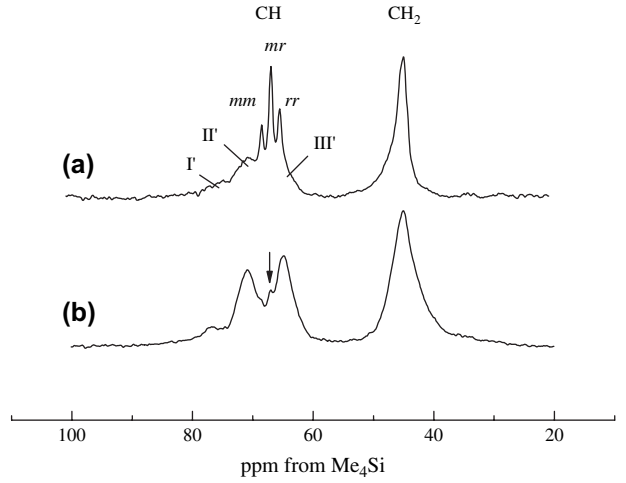

Fig. 1. High-resolution solid-state ^{13}C NMR spectra of the hydrated S-PVA films: (a) fully relaxed DD/MAS ^{13}C NMR spectrum obtained by the $\pi/4$ single sequence with a pulse delay time of 50 s and (b) CP/MAS ^{13}C NMR spectrum measured at a CP contact time of 0.8 ms. The arrow indicates the small contribution from the *mr* sequences.

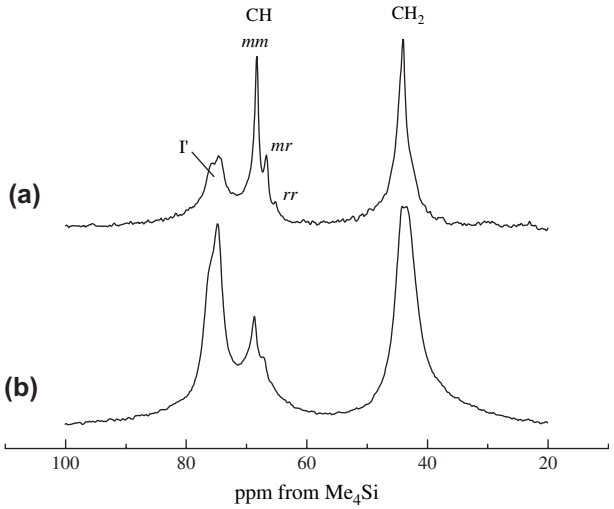

Fig. 2. High-resolution solid-state ^{13}C NMR spectra of the hydrated HI-PVA films: (a) fully relaxed DD/MAS ^{13}C NMR spectrum obtained by the $\pi/4$ single sequence with a pulse delay time of 50 s; (b) CP/MAS ^{13}C NMR spectrum.

triad sequences in the order of decreasing chemical shift value. These lines appear as a highly mobile component which is produced in the noncrystalline region by the addition of water. As already reported for solid PVA samples [14,15,21–26], the CH resonance line splits into three lines, I′, II′ and III′, which are mainly composed of the contributions from lines I, II and III in the spectrum of the crystalline component. These latter lines are, respectively, assigned to the CH carbons that are associated with two, one and no intramolecular hydrogen bond(s) in the triad sequences with the all-*trans* conformation. Lines I′ and II′ are also observed in the hydrated S-PVA sample but line III′ may be superposed on the contribution from the mobile component. In contrast, lines I′, II′ and III′ are evidently observed in the CP/MAS ^{13}C NMR spectrum as shown in Fig. 1b because the CP efficiency is much higher for the components with less molecular mobility. As for the mobile component, only a small peak as indicated by an arrow appears in this spectrum, which is ascribed to the CH carbons in the *mr* sequence. From these spectra, it is found that there are at least two components with different molecular mobilities in the hydrated S-PVA films, being in good agreement with the case for the hydrated A-PVA films [15].

Fig. 2a shows a fully relaxed DD/MAS ^{13}C NMR spectrum of the hydrated HI-PVA films with a water content of 0.72 g-H_2O/g-PVA obtained by the $\pi/4$ single sequence with a pulse delay time of 50 s. Three lines assigned to the CH carbons in the *mm*, *mr* and *rr* triad sequences are also clearly observed for the CH resonance line and their relative intensities are greatly different from those for S-PVA shown in Fig. 1a as a result of high isotacticity of HI-PVA. However, only one line that corresponds to line I′ can be observed in this sample, and this line splits into two lines in good accord with the spectrum for the dried HI-PVA sample, reflecting the features of the crystal structure of HI-PVA [14]. It is still difficult to recognize the contributions from lines II′ and III′ even in the CP/MAS spectrum shown in Fig. 2b probably due to their low mass fractions as indicated in detail later.

To obtain detailed information about the different components probably included in the hydrated stereoregular PVA films, the T_{1C} relaxation behavior has been measured for these samples at room temperature by the saturation recovery pulse sequence modified for solid-state measurements [27,28]. Fig. 3 shows the saturation recovery process of the integrated intensities of the whole CH line over the region from 55 to 85 ppm for the hydrated S-PVA films as a function of the delay time (τ) for the T_{1C} relaxation. It is clearly found by the computer-aided least-squares method that the saturation recovery curve, indicated as open squares, is composed of three components with different T_{1C} values that are designated by dotted lines. The component with the largest T_{1C} value (21.2 s) should be assigned to the crystalline component, because a larger T_{1C} value implies less molecular mobility under the present experimental condition. The component with the

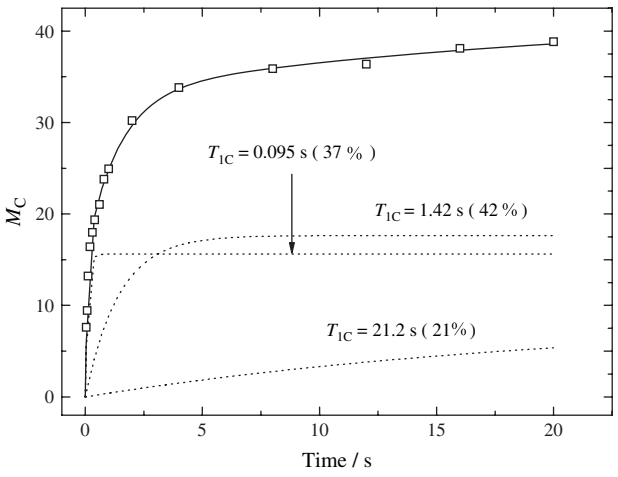

Fig. 3. The saturation recovery process of the integrated intensity for the CH resonance line of the hydrated S-PVA films as a function of the T_{1C} delay time.

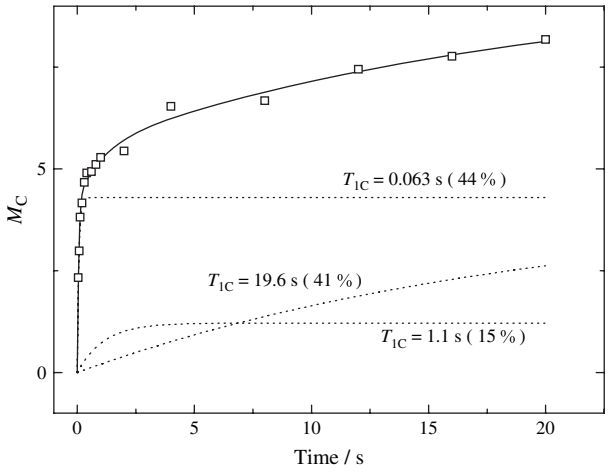

Fig. 4. The saturation recovery process of the integrated intensity for the CH resonance line of the hydrated HI-PVA films as a function of the T_{1C} delay time.

smallest T_{1C} value (0.095 s) can be readily assigned to the mobile component in the noncrystalline region because this component corresponds to the sharp CH triplet appearing at shorter relaxation delay times. In addition, the component with the medium T_{1C} value (1.42 s) is referred as the less mobile component according to a previously reported paper [15]. Since the integrated intensity is plotted against the τ value in Fig. 3, the mass fractions of the respective components, which are shown in parentheses in the figure, are also obtained by this T_{1C} analysis. The degree of crystallinity, which is estimated as mass fraction of the largest T_{1C} component, is 0.21 in this hydrated sample, while the mass fractions of the mobile and less mobile components are as considerably high as 0.37 and 0.42, respectively.

In Fig. 4, the saturation recovery process is also shown for the integrated intensity of the CH resonance line for the hydrated HI-PVA films. Similar three components with different T_{1C} values are evidently observed in this sample; the crystalline ($T_{1C} = 19.6$ s), less mobile ($T_{1C} = 1.1$ s), and mobile ($T_{1C} = 0.063$ s) components in good accord with the results for the hydrated A- and S-PVA samples. The degree of crystallinity is found to be as rather high as 0.41 in HI-PVA, whereas the mass fraction of the mobile component remains still high as 0.44. The T_{1C} values of the CH and CH_2 resonance lines thus obtained for different hydrated PVA films including A-PVA are summarized in Table 1. For comparison, the corresponding T_{1C} values are also listed for the dried stereoregular PVA films in Table 1.

The very small T_{1C} values for the mobile component appearing in all stereoregular PVA samples shown in Table 1 are due to enhanced molecular motion probably allowed by the occurrence of the rapid exchange among the hydrogen-bonded and free OH groups that are induced by the hydration in the noncrystalline region. The T_{1C} values of the crystalline components for the hydrated HI-PVA and S-PVA samples are also found to decrease to about half values of the dried samples, indicating enhancement in molecular mobility even in the crystalline region by the hydration. It should be also noted that the T_{1C} value for the hydrated A-PVA greatly decreases to 10.3 s from about 60 s for the dried sample. These results suggest that the crystalline chains of HI-PVA and S-PVA may be much more rigid than those of A-PVA even in the hydrated state because strong intramolecular or intermolecular hydrogen bonding may be successively formed along the chains for HI-PVA or for S-PVA, respectively. In fact, the CH resonance lines ascribed for the formation of these hydrogen bondings are clearly confirmed for the crystalline components in the hydrated S-PVA and HI-PVA samples as shown later in Figs. 5 and 6.

On the basis of the T_{1C} measurements shown in Figs. 3 and 4, the high-resolution ^{13}C NMR spectra of the respective components can be separately recorded mainly by using the T_{1C} filtering method. Namely, the spectra of the crystalline and mobile components were selectively obtained by the CPT1 pulse sequence [30] with $\tau = 10$ s and by the saturation recovery pulse sequence with $\tau = 0.6$ ms, respectively. Moreover, the spectrum of the less mobile component was recorded by

Table 1
^{13}C spin-lattice relaxation times of the respective resonance lines for the stereoregular PVA films measured at room temperature

Samples	T_{1C}/s			
	CH			CH_2
	I′	II′	III′	
Hydrated[a]				
HI-PVA	19.6(0.41), 1.1(0.15), 0.063(0.44)[f]			23.2(0.35), 1.3(0.25), 0.090(0.40)[f]
A-PVA[b]	10.3(0.35), 1.0(0.24), 0.04(0.41)[f]			–[e]
S-PVA	21.2(0.21), 1.42(0.42), 0.095(0.37)[f]			11.2(0.22), 0.59(0.35), 0.067(0.43)[f]
Dried[c]				
HI-PVA	41.1, 6.1	–[e]	–[e]	39.8, 4.5
A-PVA[d]	56.3, 7.2, –	59.5, 15.4, 4.7	65.2, 14.7, 3.4	65.1, 12.4, 1.9
S-PVA	–[e]	36.5, 3.8	56.7, 5.0	43.7, 4.0

[a] Obtained by the saturation recovery method.
[b] Previously obtained [15].
[c] Obtained by the CPT1 method [30].
[d] Previously obtained [26].
[e] Not estimated.
[f] The values in parentheses are the mass fractions of the respective components with different T_{1C} values.

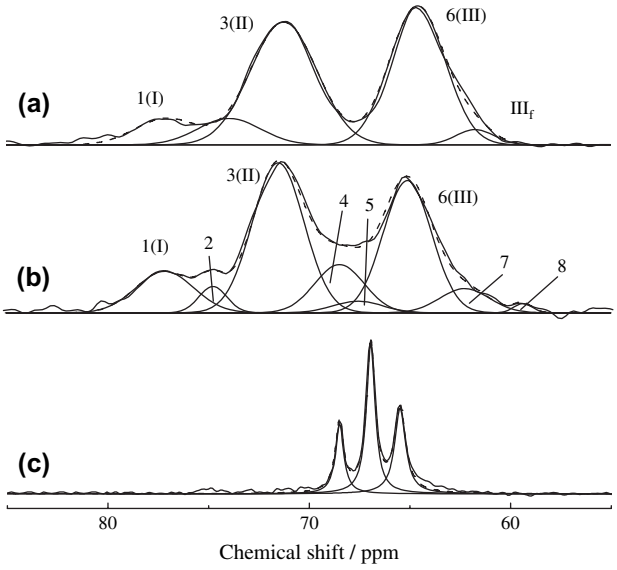

Fig. 5. High-resolution solid-state ^{13}C NMR spectra of the different components measured for the hydrated S-PVA films at room temperature: (a) crystalline, (b) less mobile, and (c) mobile.

subtracting the spectrum of the crystalline component from the spectrum measured by the CPT1 pulse sequence with $\tau = 1$ s. Fig. 5 shows the CH resonance lines for the crystalline, less mobile and mobile components thus obtained for the hydrated S-PVA films. The results of the line shape analyses are also shown for each component in this figure. Here, each constituent line was assumed to be a Gaussian for the crystalline and less mobile components according to the method that was originally established for the frozen PVA solutions [24] and successfully applied to different solid PVA samples [14,15,26,29]. In contrast, three Lorentzian curves were assumed for the triplet of the mobile component. The composite curve designated as a broken line is in good accord with the observed curve depicted by solid line in each component. As for the crystalline component shown in Fig. 5a, lines I, II and III that correspond to constituent lines 1, 3 and 6 in that line shape analysis [24], are also clearly observed in the hydrated state as expected for the chains with all-*trans* conformation. In addition, a minor Gaussian contribution referred to as III$_f$ is found to exist in the most upfield region. This contribution should be assigned to the CH carbons associated with the OH groups free from any hydrogen bonding as already reported for the hydrated A-PVA samples [15,21].

A similar line shape analysis was successfully applied to the less mobile component as shown in Fig. 5b. Interestingly, the main contributions are also lines I, II and III in this component and additional smaller lines 2, 4, 5, 7 and 8 appear as a result of the introduction of the *gauche* conformations. This fact indicates that the fraction of the *trans* conformation is considerably high in this component probably because this component may form the transitional (or interfacial) region that locates between the highly chain-oriented crystalline region and the conformationally randomized amorphous region. Accordingly, the low molecular mobility of this component in spite of addition of water may be mainly due to the restriction in conformation in the interfacial region. In contrast, the mobile component is subjected to enhanced random motion like the chains in the dissolved state, leading to the observation of the triplet ascribed to the *mm*, *mr* and *rr* sequences as shown in Fig. 5c. The respective triad fractions were determined from the integrated intensities obtained by the line shape analysis and discussed in detail later.

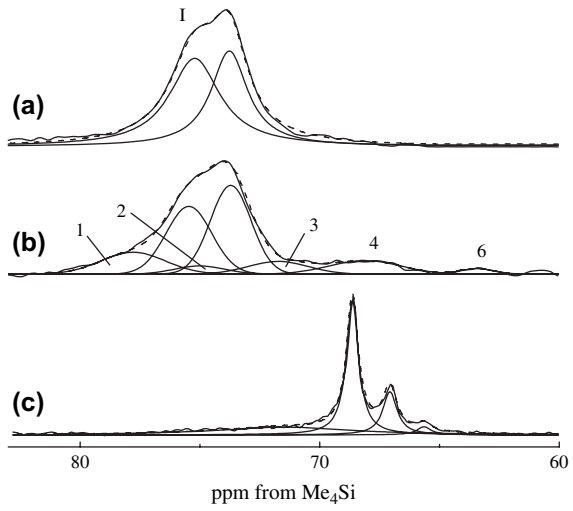

Fig. 6. High-resolution solid-state ^{13}C NMR spectra of the different components measured for the hydrated HI-PVA films at room temperature: (a) crystalline, (b) less mobile, and (c) mobile. The broad Lorentzian contribution at the downfield side is assigned to the less mobile component partially relaxed due to the relatively small T_{1C} value.

Fig. 6 shows the ^{13}C NMR spectra of similar three components separately obtained for the hydrated HI-PVA films by almost the same method used for the hydrated S-PVA sample. As shown in Fig. 6a, only line I is observed in the crystalline component in good accord with the case of the dried films [14]. This result also suggests that all OH groups are allowed to form successive intramolecular hydrogen bonding along the respective chains in the crystalline region even for the hydrated sample. Since these chains should contain some amount of *r* units even in the crystalline region, a slightly helical structure with a considerably long period may be adopted by them as previously pointed out for the dried sample [14]. Moreover, splitting of line I into two lines also suggests the existence of two types of the helical structures that may be produced in the crystalline region probably depending on the probability of the *r* units appearing along each chain [14].

As for the less mobile component shown in Fig. 6b, the CH resonance line seems very similar to that of the crystalline component including the splitting, though additional minor contributions are also observed in the downfield and upfield sides. Therefore, the line shape analysis was made by additionally introducing two contributions corresponding to the two lines in the crystalline component. However, Gaussian curves were assumed for these two lines in the less mobile component whereas Lorentzian curves were employed for the crystalline component. The composite curve indicated by the broken curve is also in good agreement with the observed curve depicted by the solid line in this case. This result

indicates that almost the same slightly helical structure should be formed in the interfacial region and the successive formation of strong intramolecular hydrogen bonding allows the formation of such a helical structure even in the hydrated state. It is also highly plausible to assume that the helical structure may be gradually disordered along each chain with increasing distance from the surface of the crystallite by the introduction of the *gauche* conformation and the breaking of successive intramolecular hydrogen bonding as a result of the salvation of water molecules. Finally, the chain segments are completely randomized in conformation and hydrogen bonding to contribute to the mobile component, which is observed as a triplet shown in Fig. 6c.

Fig. 7 shows the experimental integrated intensities (solid histograms) for the 9 constituent lines obtained for the crystalline and less mobile components of the hydrated S-PVA films by the line shape analysis shown in Fig. 5 and statistically calculated intensities (open histograms) that were obtained so as to fit the experimental intensities by the least-squares method. Here, the calculated intensities were obtained by using the equations previously derived by assuming the statistical occurrence of the *trans* and *gauche* conformations in the respective C–C bonds as well as the statistical formation of intramolecular and intermolecular hydrogen bondings in the possible successive two OH groups in the *m* or *r* units along the chain [15]. In this case, it was also assumed that almost no preferential partitioning of the *mm*, *mr* and *rr* sequences may occur in the crystalline and noncrystalline regions. This assumption is found to be reasonably held in the PVA samples used in this work as described later in detail. The calculated intensities are in good accord with the experimental intensities for both crystalline and less mobile components as shown in Fig. 7. From these statistical treatments, we can determine the optimal probabilities f_t and f_a for the occurrence of the *trans* conformation in each C–C bond and for the formation of intramolecular hydrogen bonding in the possible *m* or *r* units [15] as indicated in Fig. 7.

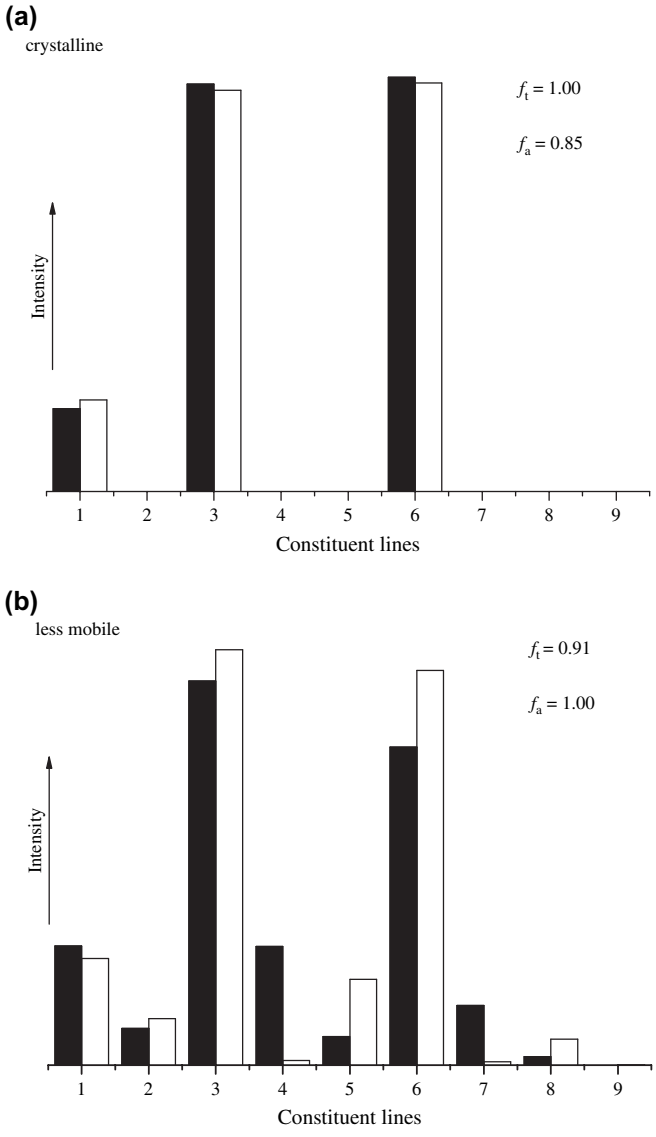

Fig. 7. Histograms for the observed and calculated relative intensities of the nine constituent lines of each component for the hydrated S-PVA films: (a) crystalline and (b) less mobile.

The f_t and f_a values obtained for the crystalline and noncrystalline components in different stereoregular PVA samples including the dried samples are listed in Table 2. However, the statistical treatment to obtain these values could not be applied to the noncrystalline or less mobile component for the hydrated and dried HI-PVA films and also for the hydrated A-PVA films probably because the chains may not adopt completely the statistical structure in conformation and hydrogen bonding in these components. As already pointed out, the f_a value is 1.0 for the crystalline component of the hydrated or dried HI-PVA films because all OH groups form intramolecular hydrogen bonding irrespective of the *m* or *r* units keeping the almost all-*trans* conformation. Such a characteristic structure may be allowed by adopting a slightly helical chain structure and seems not to be significantly influenced by the hydration. The f_a values are still as large as 0.67 and 0.80 for the crystalline components in the dried A-PVA and S-PVA films, respectively. In particular, the intramolecular hydrogen bonding tends to form at a higher probability for the two OH groups in the *m* units in the high syndiotactic chains.

Table 2
The f_t and f_a values for different components of hydrated and dried stereoregular PVA films

Samples	Crystalline		Noncrystalline	
	f_t	f_a	f_t	f_a
HI-PVA[a]				
Hydrated	1.0	1.0	–	–
Dried	1.0	1.0	–	–
A-PVA[b]				
Hydrated	1.0	0.84	–	–
Dried	1.0	0.67	0.92	0.97
S-PVA[a]				
Hydrated	1.0	0.85	(0.91)[c]	(1.0)[c]
Dried	1.0	0.80	0.82	1.0

[a] This work.
[b] Previously obtained [15].
[c] The less mobile component.

Moreover, the increase in f_a by the hydration in these crystalline components indicates that water may promote the formation of the intramolecular hydrogen bonding in the *m* units by breaking the intermolecular hydrogen bonding. This fact also implies that small amount of water molecules can penetrate into the crystalline region, as separately confirmed by the H–D exchange of the OH groups in the crystalline region observed by the immersion of the A-PVA films in D_2O [15]. In addition, such changes in hydrogen bonding will also induce the enhanced molecular motion as indicated by the decrease in T_{1C} for the hydrated films as shown in Table 1.

As for the noncrystalline components, the f_a values further increase to almost 1.0 for the dried A-PVA and S-PVA films. This indicates that the intramolecular hydrogen bonding is energetically more stable than the intermolecular hydrogen bonding in the *m* or *r* units in the dried noncrystalline region. It should be also noted that such features of hydrogen bonding seem to be also kept in the less mobile component for the hydrated S-PVA that is produced by the hydration. Moreover, the increase in f_t value to 0.91 for the less mobile component clearly supports that this component should be ascribed to the contribution from the interfacial region locating between the highly chain-oriented crystalline region and completely conformationally randomized amorphous region.

3.2. Partitioning of the mm, mr and rr units in the crystalline and noncrystalline regions

In our previous paper, dynamic viscoelasticities of different stereoregular PVA films were investigated to elucidate the effect of the stereoregularity on the molecular motion of the PVA chains [16]. The local twisting motion (β_a dispersion) and micro-Brownian motion (α_a dispersion) of the respective chains in the noncrystalline region were found to occur at almost the same temperatures for the PVA films having various stereoregularities ($mm = 0.14$–0.78). Such *mm*-insensitivity of the α_a and β_a dispersions is a somewhat great surprise because the stereoregularity would affect the mobility of the noncrystalline chains. One possible origin of the insensitivity may be the enrichment of the stereoregular units (either *m* or *r* units) of the PVA chains in the crystalline region and the resulting reduction in the difference of the stereoregularities in the noncrystalline region of the PVA samples. To examine this possibility, we estimated the mole fractions of the *mm*, *mr* and *rr* sequences for the mobile components that are produced in the stereoregular PVA films by swelling with water as described above.

The mole fractions of the *mm*, *mr* and *rr* sequences of the mobile components determined for the hydrated HI-PVA and S-PVA films are summarized in Table 3 together with the results for the hydrated A-PVA films previously obtained [15]. Here, the total values of the triad tacticities, which were determined in solution by ^{1}H NMR spectroscopy as described in Section 2, are also shown for comparison. A slight decrease in the *mm* fraction is found to occur for the mobile component in the HI-PVA films as a result of small increases in *mr* and *rr* fractions. A similar slight decrease in the *rr* fraction and a compensating increase in the *mm* fraction are also observed for the mobile component in the S-PVA films. In contrast, no appreciable changes in triad tacticities are found to occur for the mobile component in the A-PVA films. These facts indicate that a very small level of preferential partitioning of the *mm* or *rr* units tends to be, respectively, induced in the crystalline region in the highly isotactic or syndiotactic PVA films whereas almost no preferential partitioning should occur in the atactic PVA films. Nevertheless, it should be strongly pointed out that the mole fractions of the triad tacticities for the mobile components are not greatly different from the respective total values even in the HI-PVA and S-PVA films. Namely, appreciable reductions of the stereoregularity in the mobile components, which would be assumed to induce the *mm*-insensitivity of the α_a and β_a dispersions as described above, are not confirmed in these PVA samples. It is, therefore, concluded that the local twisting or the micro-Brownian motion, which is, respectively, associated with the β_a or α_a dispersion, is not significantly influenced by the stereoregularity in the PVA samples. One possible origin of the *mm*-insensitivity of the molecular motions in the noncrystalline region may be the existence of the strong intramolecular and intermolecular hydrogen bondings in the PVA films. These hydrogen bondings may make obscure the effect of the stereoregularity on the molecular mobility of PVA chains. More detailed characterization of the molecular motion in the stereoregular PVA samples will be made in relation to hydrogen bonding mainly by solid-state ^{13}C NMR in future.

Table 3
Comparison between the triad tacticities for the mobile components that are produced in different stereoregular PVA films by the addition of water and their total values

Samples		Triad tacticity		
		mm	*mr*	*rr*
HI-PVA	Total[b]	0.78	0.20	0.03
	Mobile[c]	0.70	0.26	0.04
A-PVA[a]	Total[b]	0.23	0.50	0.27
	Mobile[c]	0.24	0.50	0.26
S-PVA	Total[b]	0.14	0.48	0.38
	Mobile[c]	0.21	0.46	0.33

[a] Previously obtained [15].
[b] Determined in solution by ^{1}H NMR spectroscopy as described in Section 2.
[c] Determined for the mobile component that is produced in each sample by swelling with water as described in the text.

4. Conclusions

We have investigated the structure and hydrogen bonding for the hydrated stereoregular PVA films by solid-state ^{13}C NMR analyses, and obtained the following conclusions:

(1) Solid-state ^{13}C NMR analyses for the hydrated S-PVA and HI-PVA films reveal that there are three components with different T_{1C} values, the crystalline, less mobile and mobile components, being in good agreement with the case

for the hydrated A-PVA films. The evaluation of the T_{1C} values of the crystalline components for the hydrated films suggests that the crystalline chains of S-PVA and HI-PVA may be much rigid than those of A-PVA even in the hydrated state because strong intermolecular and intramolecular hydrogen bondings may be successively formed along the chains for S-PVA and HI-PVA, respectively.

(2) The line shape analysis of the CH resonance line for the crystalline component reveals that lines I, II and III are clearly observed in the hydrated S-PVA films as expected for the chains with all-*trans* conformation. In addition, a minor Gaussian contribution referred to as III_f, which is assigned to the CH carbons combined to the OH groups free from hydrogen bonding, is found to exist in the most upfield region. For the hydrated HI-PVA films, only line I of the CH resonance line is observed in the crystalline component in good accord with the case of the dried films. This result suggests that all OH groups are allowed to form successive intramolecular hydrogen bonding along the chains that contain some *r* units and the respective chains may adopt a slightly helical structure in the crystalline region. Moreover, splitting of line I into two lines implies the existence of two types of the helical structures that may be produced in the crystalline region probably depending on the probability of the *r* units appearing along each chain.

(3) As for the less mobile components, the line shapes of CH resonance lines for the hydrated S-PVA and HI-PVA films are, respectively, similar to those of their crystalline components, though such similarity is not clearly observed for the hydrated A-PVA films. These results indicate that almost the same structure (all-*trans* conformation for S-PVA or slightly helical structure for HI-PVA) should be mainly formed in the interfacial region because of the successive formation of strong intermolecular or intramolecular hydrogen bonding for S-PVA or HI-PVA, respectively, even in the hydrated state. In contrast, the mobile components for the hydrated S-PVA and HI-PVA films are subjected to enhanced random motion like the chains in the dissolved state, leading to the observation of the triplet ascribed to the *mm*, *mr* and *rr* sequences.

(4) In the crystalline component, the probabilities f_a of the formation of intramolecular hydrogen bonding for the hydrated and dry HI-PVA films are 1.0, and these values seem not to be significantly influenced by the hydration. For the S-PVA or A-PVA samples, the increases in f_a values by the hydration in these crystalline components are observed. These results indicate that water may promote the formation of the intramolecular hydrogen bonding in the *m* units by breaking the intermolecular hydrogen bonding.

(5) The mole fractions of the *mm*, *mr* and *rr* sequences for the mobile components are found not to greatly differ from the overall triad tacticities even for the HI-PVA and S-PVA films. It is, therefore, concluded that the local twisting or the micro-Brownian motion is not significantly influenced by the stereoregularity in the noncrystalline region of the PVA samples.

References

[1] Fujii K. J Polym Sci Part D 1971;5:431.
[2] Finch CA, editor. Polyvinyl alcohol-developments. Chichester, England: Wiley; 1992 [chapters 9 and 10].
[3] Finch CA, editor. Polyvinyl alcohol. New York, USA: John Wiley & Sons; 1973 [chapters 6 and 10].
[4] Murahasi S, Yuki H, Sano T, Yonemura U, Tadokoro T, Chatani Y. J Polym Sci 1962;62:S77.
[5] Yuki H, Hatada K, Oda K, Kinoshita H, Murahashi S, Ono K, et al. J Polym Sci Part A-1 1969;7:1517.
[6] Okamura S, Kodama T, Higashimura T. Makromol Chem 1962;53:180.
[7] Higashimura T, Suzuki K, Okamura S. Makromol Chem 1965;86:259.
[8] Murahashi S, Nozakura S, Sumi M. J Polym Sci Part B 1965;3:245.
[9] (a) Murahashi S, Nozakura S, Sumi M, Yuki H, Hatada K. J Polym Sci Polym Lett Ed 1966;4:65;
(b) Murahashi S, Nozakura S, Sumi M, Yuki H, Hatada K. Kobunshi Kagaku 1966;23:550.
[10] Ohgi H, Sato T. Macromolecules 1993;26:559.
[11] Ohgi H, Sato T. Macromolecules 1999;8:2403.
[12] Ohgi H, Sato T. Polymer 2002;43:3829.
[13] Horii F, Hu S, Deguchi K, Sugisawa H, Ohgi H, Sato T. Macromolecules 1996;29:3330.
[14] Ohgi H, Sato T, Hu S, Horii F. Polymer 2006;47:1324.
[15] Masuda K, Kaji H, Horii F. Polym J 2001;33:356.
[16] Ohgi H, Sato T, Watanabe H, Horii F. Polym J 2006;38:1055.
[17] Yamamoto T, Yoda S, Takase H, Sangen O, Fukae R, Kamachi M, et al. Polym J 1991;23:185.
[18] Moritani T, Kuruma I, Shibatani K, Fujiwara Y. Macromolecules 1972;5:577.
[19] DeMember JR, Haas HC, MacDonald RL. J Polym Sci Polym Lett Ed 1972;10:385.
[20] Horii F, Hirai A, Kitamaru R, Sakurada I. Cellul Chem Technol 1985;19:513.
[21] Horii F, Hu S, Ito T, Odani H, Kitamaru R, Matsuzawa S, et al. Polymer 1992;33:2299.
[22] Hu S, Horii F, Odani H, Narukawa H, Akiyama A, Kajitani K. Kobunshi Ronbunshu 1992;49:361.
[23] Hu S, Tsuji M, Horii F. Polymer 1994;35:2516.
[24] Masuda K, Horii F. Macromolecules 1998;31:5810.
[25] Masuda K, Kaji H, Horii F. Polym J 1999;31:105.
[26] Masuda K, Kaji H, Horii F. J Polym Sci Part B Polym Phys 2000;38:1060.
[27] Kitamaru R, Horii F, Murayama K. Macromolecules 1986;19:636.
[28] Hirai A, Horii F, Kitamaru R, Fatou JG, Bello A. Macromolecules 1990;23:2913.
[29] Yang H, Hu S, Horii F, Endo R, Hayashi T. Polymer 2006;47:1995.
[30] Torchia DA. J Magn Reson 1978;30:613.